Conf-9410254--1
SAND 94-2639C

Nonequilibrium Multiphase Mixture Modeling of Energetic Material Response (U)

M. R. Baer, Eugene Hertel and Raymond Bell
Sandia National Laboratories, Albuquerque, New Mexico 87185 USA*

To model the shock-induced behavior of porous or damaged energetic materials, a nonequilibrium mixture theory has been developed and incorporated into the shock physics code, CTH[3]. Foundation for this multiphase model is based on a continuum mixture formulation given by Baer and Nunziato.[1] In this nonequilibrium approach, multiple thermodynamic and mechanics fields are resolved including the effects of material relative motion, rate-dependent compaction, drag and heat transfer interphase effects and multiple-step combustion. Benchmark calculations are presented which simulate low-velocity piston impact on a propellant porous bed and experimentally-measured wave features are well replicated with this model. This mixture model introduces micromechanical models for the initiation and growth of reactive multicomponent flow which are key features to describe shock initiation and self-accelerated deflagration-to-detonation combustion behavior. To complement one-dimensional simulation, two dimensional numerical simulations are presented which indicate wave curvature effects due to the loss of wall confinement.

Introduction

Hazards analysis for weapon systems safety and surety assessment considers a variety of accidental scenarios whereby impact conditions can lead to direct shock initiation or other modes of combustion such as deflagration-to-detonation transition (DDT) and delayed detonation (XDT). These modes of combustion can self-accelerate into detonation due to the behavior of the energetic material microstructure at internal boundaries. The coupled thermal/chemical/mechanical response of these features are the key issues for assessing the violence of reaction resulting from combustion of the energetic material.

A continuum multiphase model has been posed which well describes the self-accelerated combustion of granular materials as demonstrated in references 1 and 2. A variety of energetic materials, including explosives and propellants, has been experimentally and theoretically studied to provide a foundation for simulation in multidimensional analyses. This multiphase model has been recently incorporated into the Sandia shock physics code - CTH[3]. The interaction of rapid combustion with deformable confinement is a critical aspect of sustained accelerated combustion; thus, simulation of real systems requires the capability of multidimensional, multi-material large deformation, strong shock wave physics.

In the sections to follow, the mixture formulation is outlined and its numerical implementation into the CTH shock physics code is described. Then, one and two-dimensional simulations are discussed which provide a benchmark for the nonequilibrium mixture theory.

*This work performed at Sandia National Laboratories supported by the U.S. Department of Energy under contract DE-ACO4-94AL85000

Theoretical Foundation

The equations of motion for a multiphase mixture are outlined in this section and recast to a finite volume formulation for shock physics analyses. The full derivation of this description is not repeated here; hence only the final forms of the conservation laws are described. Mixture theory is based on the concept that separate phases simultaneously occupy regions of space. Thus, a multiphase material possesses independent thermodynamic and kinematic fields. Multiple balance laws are used to describe a locally averaged thermal, mechanical and chemical response of a collection of condensed phases or gas-filled pores. In contrast to single phase continuum mechanics, a mixture average for a multiphase flow includes the effects of internal boundaries (or phase interfaces) across which the interchange of mass, momentum and energy takes place. These important microscale models are the new features of the multiphase description in the shock physics code, CTH.

Modern developments of continuum mixture theory provides the framework for a thermodynamically-consistent description of nonequilibrium processes of fully-compressible reactive mixtures. A unique feature of this description is the treatment of volume fractions as independent kinematic variable allowing compressibility of all phases without any compromise on compaction behavior. Specifically, the theory of reactive mixtures is firmly based on establishing balance equations using the Second Law of Thermodynamics in the determination of admissable constitutive relationships for a system of multiphase equations that are well-posed[4].

To simplify the discussion of mixture theory, consider a region in space that is occupied by two phases (denoted by subscript a) - condensed (subscript s) and gas (subscript g). At some appropriate scale, each phase is viewed as occupying every spatial location in the field. Physically, this is not the case since each phase occupies a volume distinct from the other. Thus, to represent the discrete nature of the mixture, each phase is assigned independent thermodynamic and kinematic states. At each point a phase material density, $\gamma_a(x,t)$, is defined representing the mass per unit volume occupied by each phase and the space displaced by that phase is the volume fraction, $\phi_a(x,t)$. (The volume fraction is a relative fraction of space occupied by material regardless of material type - the fraction of space treated as void is excluded.) Of the fraction of space occupied by the mixture, saturation implies that $\sum\phi_a = 1$ and the density of the local mixture is the sum of partial densities, $\rho_a = \gamma_a\phi_a$, or: $\rho = \sum\rho_a$.

In generalized mixture theory, each phase is assigned independent velocities, $\vec{v}_a = \vec{v}_a(x,t)$, and the conservation equations for each phase are expressed as:

Mass: $$\dot{\rho}_a = -\rho_a\nabla\cdot\vec{v}_a + \dot{c}_a^{\dagger} \quad (1)$$

Momentum: $$\rho_a\dot{\vec{v}}_a = \nabla\cdot\underline{\sigma}_a + \rho_a\vec{b}_a + \vec{m}_a^{\dagger} - \dot{c}_a^{\dagger}\vec{v}_a \quad (2)$$

Energy: $$\rho_a\dot{e}_a = \underline{\sigma}_a:\vec{\nabla}\vec{v}_a + \rho_a r_a + e_a^{\dagger} - (\vec{m}_a^{\dagger} - \dot{c}_a^{\dagger}\vec{v}_a)\cdot\vec{v}_a - \dot{c}_a^{\dagger}\left(e_a + \frac{\vec{v}_a\cdot\vec{v}_a}{2}\right) \quad (3)$$

By definition, the Lagrangian material derivative is given as: $\dot{f}_a = \partial f/\partial t + \vec{v}_a\cdot\nabla f$. In these conservation equations, $\dot{c}_a$ is the mass exchange between phases due to chemical reaction, $\vec{b}_a$ is the external body force, $\vec{m}_a$ is the momentum exchange resulting from the forces acting on phase boundaries, e_a is the internal energy of each phase, r_a is the external energy source, and e_a includes the energy exchange due to heat transfer and the irreversible work done at phase boundaries. The symmetric stress tensor, $\underline{\sigma}_a$, is expressed in terms of the phase pressure, p_a, and the shear stress $\underline{\tau}_a$; thus $\underline{\sigma}_a = -\phi_a p_a\underline{I} + \underline{\tau}_a$ where $tr(\underline{\tau}_a) = 0$.

Consistent with the derivations used in mixture theory, summation of each balance equation over all phases yields the response of the total mixture corresponding to the well known equations of motion for a single phase material. The following constraints are imposed on the phase interactions: $\sum\dot{c}_a^{\dagger} = 0$, $\sum\vec{m}_a^{\dagger} = 0$, and $\sum e_a^{\dagger} = 0$. The total mixture equations (the identical balance laws solved in CTH) are given (in Eulerian form) as follows:

Total Mass: $$\dot{\rho} = -\rho\nabla\cdot v \quad (4)$$

Total Momentum: $$\rho\dot{\vec{v}} = \nabla\cdot\underline{\sigma} + \rho\vec{b} \quad (5)$$

Total Energy: $$\rho\dot{e} = \underline{\sigma}:\vec{\nabla}\vec{v} + \rho r \quad (6)$$

where the overdot denotes the mixture material derivative. By definition, the mixture velocity is the barycentric (mass averaged) velocity defined as: $\vec{v} = \sum\rho_a\vec{v}_a/\rho$ and the phase diffusion velocity (discussed later in this section) is given as $\vec{u}_a = \vec{v}_a - \vec{v}$.

In considering two phases, the restrictions from the Second Law of Thermodynamics suggest admissable forms of phase interaction. For the sake of brevity, the algebraic manipulation will not be repeated here and the final forms of these interactions are given as follows:

Mass Exchange $$\dot{c}_s^{\dagger} = -\dot{c}_g^{\dagger} \quad (7)$$

Momentum Exchange

$$\vec{m}_s^{\dagger} = -\vec{m}_g^{\dagger} = \delta(\vec{v}_g - \vec{v}_s) + \dot{c}_s^{\dagger}\vec{v}_i + p_i\nabla\phi_s \quad (8)$$

Energy Exchange

$$e_s^{\dagger} = -e_g^{\dagger} = \vec{m}_s^{\dagger}\cdot\vec{v}_s + h(T_g - T_s) + \dot{c}_s^{\dagger}\left(e_i - \frac{v_s^2}{2}\right) + W_i^{\dagger} \quad (9)$$

where the interfacial velocity is defined as, $\vec{v}_i = (\vec{v}_s + \vec{v}_g)/2$, the interfacial surface stress is $p_i = p_g$, the interfacial total energy is $e_i = e_s$ and the dissipative compaction work is defined as: $W_i^{\dagger} = -(p_s - \beta_s)\cdot\left(\dot{\phi}_s - \dot{c}_s^{\dagger}/\gamma_s\right)$. The momentum and energy exchange coefficients representing microscale boundary layer effects, δ and h, are modeled as functions of local flow conditions and specific surface area. Finally, after including appropriate equations of state for each phase, closure is obtained by imposing a rate description for volume fraction consistent with the Second Law of Thermodynamics. The evolutionary equation for solid volume fraction is

$$\dot{\phi}_s - \dot{c}_s^{\dagger}/\gamma_s = \frac{\phi_s\phi_g}{\mu_c}(p_s - p_g - \beta_s) \quad (10)$$

where the intragranular stress, β_s is defined and the rate of volume fraction change is controlled by the compaction viscosity, μ_c . It is noted that this nonequilibrium multiphase description is somewhat different than that previously implemented in CTH as the multiple pressure and temperature model. This description implies a slightly different set of mixture rules because the volume fraction is treated as an independent kinematic variable. With this new

DISCLAIMER

DISCLAIMER

Portions of this document may be illegible in electronic image products. Images are produced from the best available original document.

formulation there is no requirement to renormalize energies and the local pressure remains a volume fraction-weighted average of individual phase pressures. The rate of change of volume fraction is related directly to the local state of pressure nonequilibrium and includes the effects of combustion.

Having established the general equations of motion for a two-phase description, the model equations are given in a form consistent with the shock physics modeling in CTH. To recast the equations of motion into integral form, the Lagrangian material derivative is defined as: $d/dt = \partial/\partial t + \dot{\mathbf{v}} \cdot \nabla$ and

$$\frac{d}{dt}\int_{\beta} f dV = \int_{\beta}\frac{\partial f}{\partial t} dV + \oint_{\partial\beta} f \dot{\mathbf{v}} \cdot dA .$$

Following algebraic manipulation, equation (1), for the gas phase mass conservation, is redefined as:

$$\frac{d}{dt}\int_{\beta} \rho_g dV = -\int_{\beta} \dot{c}_s^{\dagger} dV - \oint_{\partial\beta} \rho_g \dot{\mathbf{u}}_g \cdot dA \qquad (11)$$

Simply stated, this equation expresses that the time rate of change of gas mass equals the rate of mass generation as the solid phase decomposes to a gas minus the diffusion of gas mass in (or out of) the mixture-averaged volume.

In a similar transformation, the gas momentum conservation equation is recast into the following integral form:

$$\begin{aligned}\frac{d}{dt}\int_{\beta} \rho_g \dot{\mathbf{v}}_g dV = &-\oint_{\partial\beta} \hat{\mathbf{n}} \cdot (\phi_g p_g \underline{I})\, dA + \\ &\int_{\beta} \rho_g \hat{\mathbf{b}}_g dV - \int_{\beta} \dot{\mathbf{m}}_s dV^{\dagger} - \oint_{\partial\beta} \rho_g \dot{\mathbf{v}}_g \dot{\mathbf{u}}_g \cdot dA\end{aligned} \qquad (12)$$

This equation states that the rate of change of gas momentum is balanced with the pressure forces, body forces, interphase momentum exchange (such as drag) and the last term corresponds to the diffusion of momentum into (or out of) the mixture-averaged volume.

For gas energy conservation, it is convenient to resolve the total gas energy, $E_g = e_g + (\dot{\mathbf{v}}_g \cdot \dot{\mathbf{v}}_g)/2$, and the integral balance equation for gas phase energy is given as:

$$\begin{aligned}\frac{d}{dt}\int_{\beta} \rho_g E_g dV = &-\oint_{\partial\beta} \hat{\mathbf{n}} \cdot (\dot{\mathbf{v}}_g \phi_g p_g)\, dA - \\ &\oint_{\partial\beta} \hat{\mathbf{n}} \cdot (\dot{\mathbf{u}}_g \rho_g E_g)\, dA + \int_{\beta} (S_g - \dot{e}_s^{\dagger})\, dV\end{aligned} \qquad (13)$$

where, in the above balance laws for gas phase momentum and energy, the stress matrix has been simplified to the form: $\underline{\sigma}_g = -\phi_g p_g \underline{I}$, and the energy source includes the body forces: $S_g = \dot{\mathbf{v}}_g \cdot \rho_g \hat{\mathbf{b}}_g + \rho_g r_g$. This integral equation then states that the rate of change of gas energy (including gas phase kinetic energy) is balanced by the work done by the gas pressure forces, the diffusion of gas energy into (or out of) the mixture-averaged volume and the volumetric energy gain (or loss) due to sources and the interphase exchange of energy occurring at phase boundaries.

To transform Equation 10 into appropriate integral form, it is convenient to resolve the solid phase material density field using the solid phase mass conservation equation. After some algebraic manipulation, this field equation is given as:

$$\frac{d}{dt}\int_{\beta} \gamma_s dV = -\int_{\beta} \gamma_s \frac{(1-\phi_s)}{\mu_c}(p_s - p_g - \beta_s)\, dV - \oint_{\partial\beta} \gamma_s \dot{\mathbf{u}}_s \cdot dA \qquad (14)$$

In general, additional rate equations of the form: $\partial f_a/\partial t + \dot{\mathbf{v}}_a \cdot \nabla f_a = \dot{f}_a$ transform to an integral equation using the phase mass conservation equation (1) yielding:

$$\frac{d}{dt}\int_{\beta} \rho_a f_a dV = \int_{\beta} (\rho_a \dot{f}_a^{\dagger} + f_a \dot{c}_a^{\dagger})\, dV - \oint_{\partial\beta} \rho_a f_a \dot{\mathbf{u}}_a \cdot dA \qquad (15)$$

All of the details to the combustion description, momentum and energy phase interaction and additional heat transfer relationships are given in References 1 and 2. For a two-phase mixture, the velocity components for only one phase and the mixture average need to be resolved. Thus, if the gas phase and mixture averaged velocities are known then the solid phase velocity and the solid phase diffusion velocity are defined as $\dot{\mathbf{v}}_s = (\rho \dot{\mathbf{v}} - \rho_g \dot{\mathbf{v}}_g)/(\rho - \rho_g)$ and $\dot{\mathbf{u}}_s = \rho_g (\dot{\mathbf{v}} - \dot{\mathbf{v}}_g)/(\rho - \rho_g)$.

Numerical Implementation

The shock physics code, CTH, is a multimaterial multidimensional Eulerian finite volume code which serves as the platform for implementing the reactive multiphase mixture model. Details of the base code and its material models are not given here and the interested reader is referred to references 5 and 6 for such information.

The current version of CTH uses an Eulerian mesh which is fixed in space. Mixture-averaged conservation equations, in finite volume form, are solved in a Lagrangian step and distorted cells are remapped back to a fixed mesh. In addition to overall conservation equations, internal state variables are solved for various material models[7].

In incorporating the mixture theory it is important to note that the overall mixture quantities are never modified, thus conservation of mass, momentum and energy for the total system is preserved. Mixture rules dictate how these quantities are proportioned amongst various phases. Additionally, the local flow velocity is recognized as being a mass-averaged quantity.

The phase conservation equations, given by Equations 11-15, have a common mathematical structure. All of these equations have source and phase diffusion terms. The phase diffusion terms represent advection in or out of the cells following phase diffusion velocity fields. Incorporating these effects is done using operator splitting whereby all phase quantities are diffused in or out of cells then the phase quantities are allowed to interact during the Lagrangian step. The methodology of this approach is based on earlier work given in reference 8.

During the transportive step, a Flux-Corrected Transport (FCT)[9] method is used and internal boundary conditions are incorporated with a variant of virtual cell embedding (VCE)[10]. This positivity-preserving high order algorithm does not introduce artificial smearing at material interfaces. It is to noted that for shocked flows, phase diffusion quantities are weak and significant only in boundary layer regions.

Typical of multiphase simulation, the interactions of phases occur with greatly disparate time-scales and thus sources are mathematically stiff. Since explicit time differencing (even with subcycling) is inaccurate, an algorithm based on asymptotic semi-analytical solutions is used for phase interaction[11]. As expected, the internal state variables related to the local volume fractions must be accurately resolved to preserve consistency of the numerical solutions. Following the Lagrangian step, the volume fractions for the single mixed phase material are mapped into a single field which then passed into the remap step. These quantities are subsequently reassembled for equation of state evaluation for the next time step. Thus, sound speed constraints are brought into place for evaluation of Courant conditions.

In the next section, a benchmark numerical solution is discussed in which shock induced reaction is induced in a porous propellant bed. Although phase diffusion effects are minor, strong phase interactions occur which provides a good test of the proposed numerical strategy.

Low Velocity Impact Simulations

One and two-dimensional numerical simulations of a piston-driven low velocity impact on a porous bed of energetic material are conducted which replicate conditions in a experiment done by Sandusky, et al[12]. A pictorial of this experiment is shown in figure 1. A gas driven piston impacts on a bed of NC/NG based propellant confined in a cylindrical tube geometry.

Following impact, a compaction wave is produced and high strain rate at the compaction front triggers multiphase combustion. This unstable process leads to rapid combustion and the formation of a fast

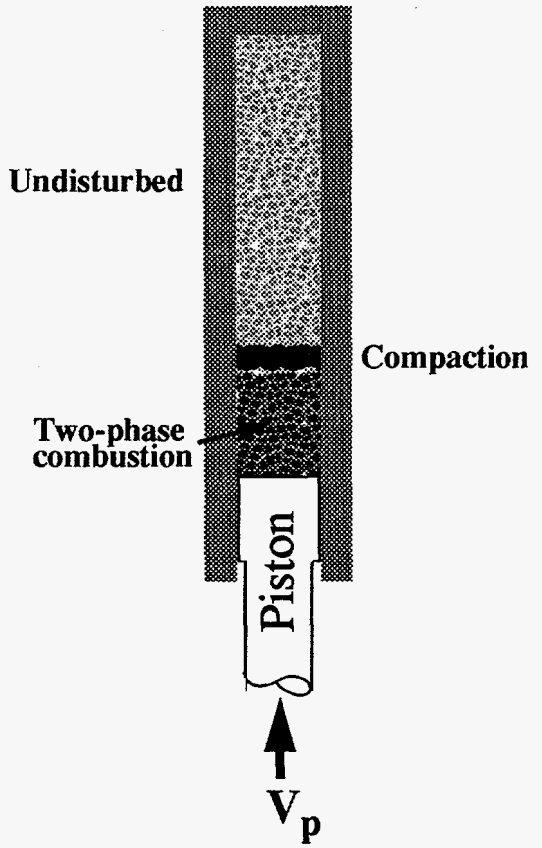

Figure 1. Piston driven compaction experiment in granular propellent porous bed.

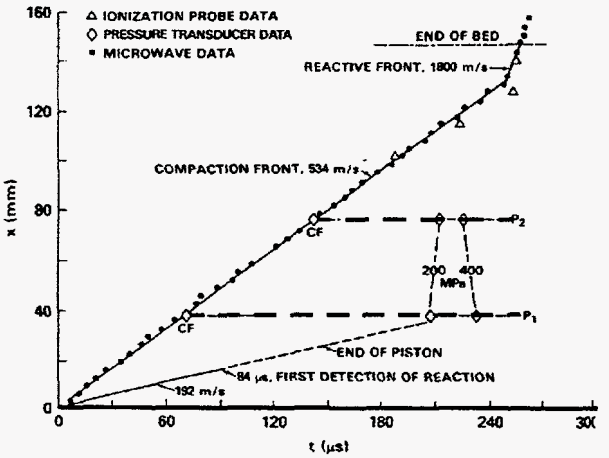

Figure 2. Experimental trajectories of wave fronts following a 190 m/s impact on a granular ball propellant bed.

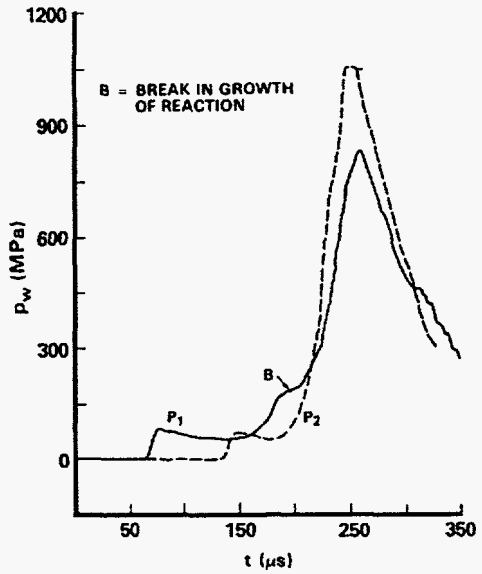

Figure 3. Pressure gauge measurements at two locations along the confined porous propellant bed.

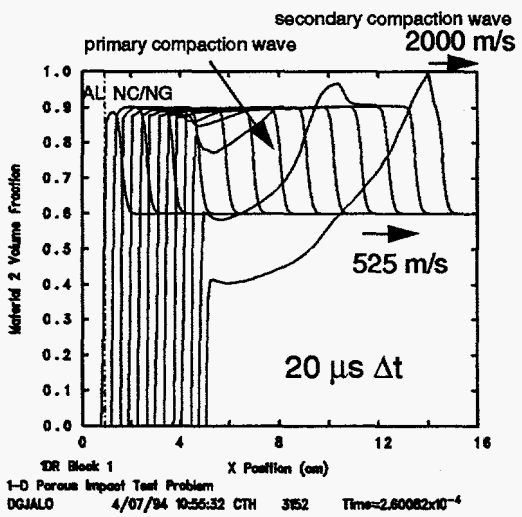

Figure 4. Overlay of volume fraction wave fields for a 190 m/s impact.

deflagration wave and shock formation. The interaction of compaction and multistage combustion is clearly a complex wave process.

In the experimental studies by Sandusky and colleagues, numerous diagnostics were used to resolve various wave features[13]. Most importantly, the compaction wave front was probed using microwave interferometry and pressure gauges were used to determine various wave fields. Figure 2 displays the trajectory of the compaction wave following a 190 m/s impact measured using microwave interferometry. It is to be noted that an abrupt change in wave speed was observed well removed from the piston/propellant interface.

Figure 3 displays several pressure gauge records at given location along the tube confinement wall. A weak compaction front is observed followed by the onset of rapid pressurization.

One dimensional simulations of this experiment using the multiphase mixture model in CTH is displayed in the subsequent figures that replicate all of the features observed in the experimental study. Figure 4 displays an overlay of the volume fraction of the solid phase reactant. Numerical simulation shows a dispersive compaction wave originating from the piston/bed interface and moves at a velocity consistent with the experimental observation.

As a result of high strain rate at the dispersive compaction front, low level of reactivity is induced whereby pyrolysis combustion products are formed in an induction zone. After approximately 100μs delay, energy release in the gas phase takes place as pyrolysis products are converted to final stage combustion gases. A secondary compaction wave is formed and is supported by the reaction. When heat transfer conditions are sufficient to trigger grain burning, very rapid pressurization occurs. Eventually, the combustion wave coalesces with the primary compaction wave and an apparent abrupt change in wave speed occurs. Details of the pressurization field is shown in figure 5.

As a demonstration of the importance of treating pressure nonequilibrium, figure 6 displays only the gas phase component of the principle stress. In the early stages of reaction, greatly disparate pressure fields evolve. Much of the initial stresses of the primary compaction wave is supported by the solid reactant material; later, it is the gas phase pressure which supports the combustion driven reactive compaction wave.

In figures 7 and 8, the temperature fields are shown for the gas and solid phases, respectively. As expected, greatly different temperatures arise because much of the energy release occurs in the gas phase. The effects of multistage combustion are clearly evident. Figure 8, weak compressional heating occurs early and

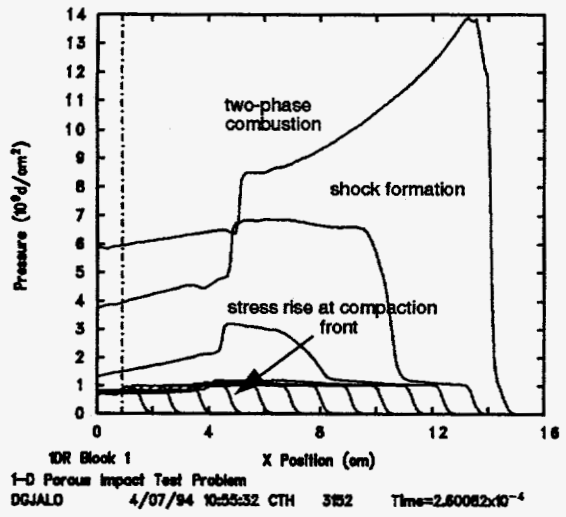

Figure 5. Overlay of pressure wave fields during impact and subsequent reaction

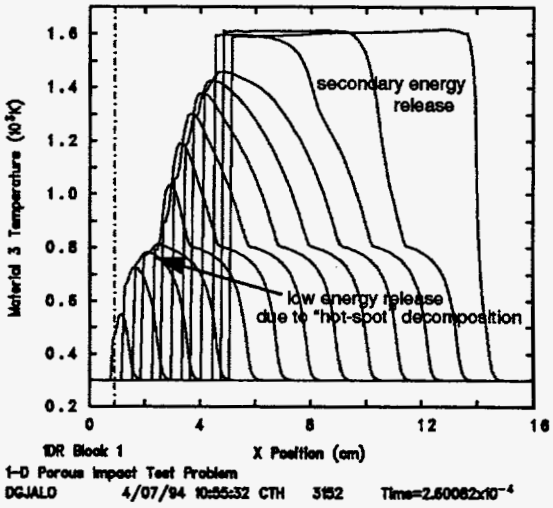

Figure 7. Overlay of gas phase temperatures in one-dimensional CTH simulation of low velocity impact.

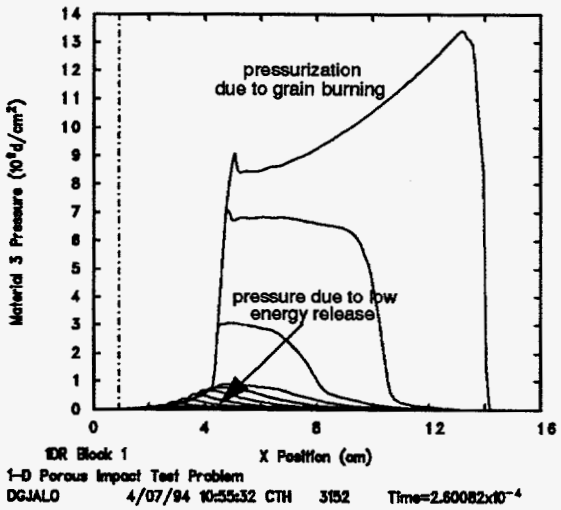

Figure 6. Gas phase pressures at 20 ms intervals during compaction and reaction.

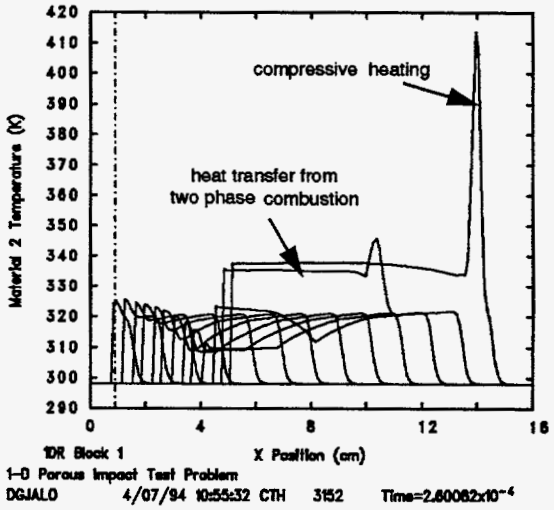

Figure 8. Overlay of solid reactant phase temperatures in one-dimensional CTH simulation of low velocity impact.

later during gas phase pressurization heat transfer enhances the heatup of the solid phase. Additional compressional heating takes place as the supported secondary compaction wave strengthens to a shock.

In similar experimental studies conducted at LANL by McAfee, et al.[14] thin wall tubes were used and that release of confinement near the burning region auggested the formation of multiple "shocks" prior to the onset of rapid burning. These observations are based on sequential x-ray radiographs. Only gross features of the wave fields were measured in these experiments, hence interpreted wave behavior is speculative.

A two-dimensional simulation of a weakly confined column of propellant is presented as a preliminary numerical simulation of these piston impact experiments. A thin-walled steel tube, confining NC/NG propellants, is modeled at with impact conditions similar to the previous one-dimensional simulations. Figure 9 displays three 50 μs time interval following the low velocity impact. In these CTH output plots, materials are rendered on the right half of the plots and color contours of the solid phase volume fraction is shown on the left half image plane. Low to high reactant volume fraction contours corresponds from blue to red variations, respectively.

At these early times following impact, it is seen that a curved compaction wave evolves as the lateral release from the wall takes place. The compaction wave is weakly supported and the weakened pressure field lessens the extent of reaction. At a later time, (not displayed here due to space limitations), reaction is seen to first arise near the center of the column and a radial wave appears which leads to the secondary compaction wave. As this wave interacts with the confinement a secondary release takes place and sustained reaction greatly depends on the pressurization from low level combustion competing with the dissipation by rarefaction of confinement release. As expected, the interaction with the combustion reactions and compaction fields in multidimensional simulation is strongly influenced by the effects of confinement and simulation of the LANL experiments may lead to a bettere understanding of multidimensional behavior.

Future work is planned to simulate these low velocity experiments for a granular bed of HMX explosive. Additionally, statistical crack fracture models are being incorporated into CTH and the reactive multiphase mixture model will be coupled to address simulation of delayed detonation. Additionally, mixture theory is being formulated to treat more than two phases and this is be incorporated as an extension of multiphase predictive capabilities.

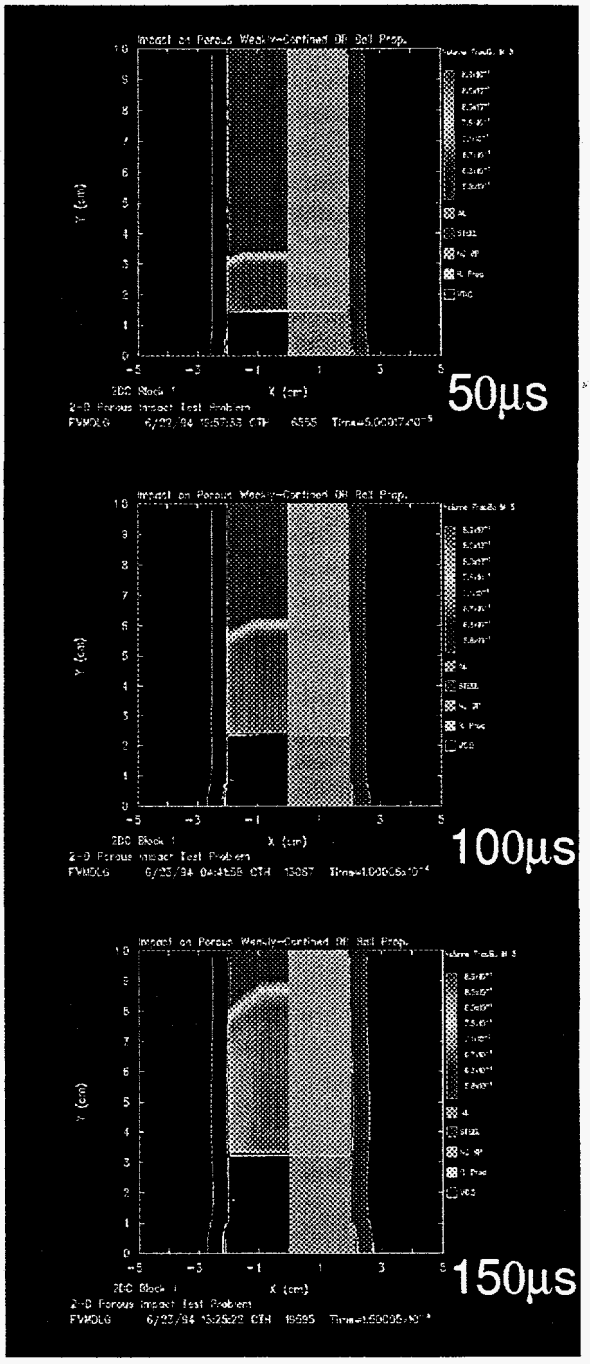

Figure 9. Two-dimensional CTH simulations of low velocity impact of a weakly confined porous column of propellant. Split images correspond to materials on right and solid phase volume fraction contours on left.

Summary

A nonequilibrium multiphase mixture model has been described in this paper which has been implemented into shock physics analysis. The effects of strong phase interaction including combustion, momentum and energy exchange are included by allowing mixed phases to have relative velocities and independent thermal and stress fields. An operator splitting methodology is described for numerical implementation of this model.

Preliminary benchmarks of this mixture approach has addressed low-velocity impact experiments in one and two-dimensional simulations. All of the observed reactive wave behavior are replicated by the modeling. Multidimensional simulation can serve as an important numerical diagnostic for probing the nature of complex wave fields. Future work is aimed toward using this tool with experimental studies of energetic material response to enhance predictive capabilities for weapon safety and surety assessment.

References

1. Baer, M. R. and Nunziato, J. W., "*A Two-Phase Mixture Theory for Deflagration-to-Detonation Transition (DDT) in Reactive Granular Materials*," **International Journal of Multiphase Flow**, Vol. 12, 1986, pp 861-889.

2. Baer, M. R. and Nunziato, J. W.,"*Compressive Combustion of Granular Materials Induced by Low-Velocity Impact*," **Ninth Symposium (International) on Detonation**, OCNR 113291-7, 1989, pp 293-305.

3. McGlaun, J. M., Thompson, S.L., Kmetyk, L. N. and Elrick, M.G., "*A Brief Description of the Three-Dimensional Shock Wave Physics Code CTH*," Sandia National Laboratories, SAND89-0607, 1990.

4. Embid, P. and M. R. Baer, "Mathematical Analysis of a Two-Phase Continuum Mixture Theory", **Continuum Mechanics and Thermodynamics**, Vol 4, 1992, pp 279-312.

5. McGlaun, J. M., "*CTH Reference Manual: Lagrangian Step for Hydrodynamic Materials*" Sandia National Laboratories, SAND90-2645, 1990.

6. McGlaun, J. M., "*CTH Reference Manual: Cell Thermodynamics*," Sandia National Laboratories, SAND91-0002, 1991.

7. Kerley, G. I., "*CTH Equation of State Package: Porosity and Reactive Burn Models*", Sandia National Laboratories, SAN92-0553, 1992.

8. Gross, R. J., and M. R. Baer,"*A Study of Numerical Solution Methods for Two-Phase Flow*," Sandia National Laboratories, SAND84-1633, 1986.

9. Boris, J. P., A. M. Landsberg, E. S. Oran, and J.H. Gardner, "*LCPFCT- A Flux-Corrected Transport Algorithm for Solving Generalized Continuity Equations*", Naval Research Laboratory, NRL/MR/6410-93-7192, 1993.

10. Landsberg, A. M., J. P Boris, T. R. Young and R. J. Scott, "*Computing Complex Shocked Flows Through the Euler Equations*," **Proceeding of the 19th International Symposium on Shock Waves**, University of Provence, Marseille, France, 1993.

11. Oran, E. S. and J. P. Boris, **Numerical Simulation of Reactive Flow**, Elsevier, pp 134-180., 1987.

12. Sandusky, H. W. and R. R. Bernecker, "*Compressive Reaction in Porous Beds of Energetic Materials*," **Eighth Symposium (International) on Detonation**, NSWC MP 86-194, 1985, pp. 881-891.

13. Glancy, B. C., H.W. Sandusky, P. J. Miller and A. D. Krall, "*Dynamic Compaction and Compressive Reaction Studies for Single and Double-base Ball Propellants*," **Ninth Symposium (International) on Detonation**, OCNR 113291-7, 1989, pp 341-353

14. McAfee, J. M., B. W. Assay, A. W. Campbell and J. B. Ramsay, "*Deflagration to Detonation in Granular HMX*," **Ninth Symposium (International) on Detonation**, OCNR 113291-7, 1989, pp 256-279.